Polarization dependence of Schottky barrier heights at interfaces of ferroelectrics determined by photoelectron spectroscopy

Feng Chen* and Andreas Klein

Technische Universität Darmstadt, Institut für Materialwissenschaft, Fachgebiet Oberflächenforschung, Petersenstraße 32, D-64287 Darmstadt, Germany

(Received 6 January 2012; revised manuscript received 24 August 2012; published 5 September 2012)

Ferroelectric polarization in thin films is stabilized by screening charges in the metal electrodes. Imperfect screening of the polarization charge strongly modifies the film's capacitance and should lead to a variation of the Schottky barrier height at the interface with polarization direction. An experimental approach based on photoelectron spectroscopy is introduced which allows us to quantitatively determine Schottky barrier heights at ferroelectric/metal interfaces in dependence on polarization. The procedure is exemplified for $BaTiO_3$ single crystals with RuO_2 and Pt electrodes, revealing a variation of Schottky barrier height of 1.1 and 0.65 eV in dependence on polarization for RuO_2 and Pt electrodes, respectively. Inhomogeneous barrier switching is observed for Pt electrodes, which may be related to defect formation during metal deposition.

DOI: 10.1103/PhysRevB.86.094105 PACS number(s): 77.80.Fm, 73.30.+y, 77.84.Cg, 79.60.Jv

I. INTRODUCTION

Ferroelectric materials are characterized by their spontaneous electric polarization. In perovskite materials like $BaTiO_3$ this is caused by ionic displacement.[1] The depolarizing electric field associated with the bound charges, which occur at surface or interface planes where the polarization has a perpendicular component, must be screened in order to stabilize polarization.[2] Domain formation and compensating charges are predominant screening mechanisms. Most straightforward is screening by the induced charges in a metallic electrode. The screening of ferroelectric polarization by metallic electrodes depends, however, strongly on the details of the atomic configuration at the interface. Imperfect screening leading to additional interfacial capacitances may occur but ferroelectricity may also be enhanced for certain interfacial configurations.[3,4] In the case of imperfect screening of the polarization by metal electrodes, the Schottky barrier height Φ_B at the ferroelectric/metal interface is expected to depend strongly on the magnitude and orientation of polarization.[5]

The difference in barrier height expected for polarization reversal is given by

$$\Delta\Phi_B = 2\lambda_{eff} \cdot (D_S/\varepsilon_0), \quad (1)$$

where D_S, ε_0, and λ_{eff} are the dielectric displacement in the ferroelectric, the vacuum permittivity, and the effective screening length, respectively. The latter quantity depends on the charge density distribution at the interface, determined by the atomic configuration. For interfaces of $BaTiO_3(100)$ with $SrRuO_3$ (SRO) and Pt, the values predicted by Stengel *et al.* are $\Delta\Phi_B = 1.8$ eV for SRO and 0.03 eV for Pt electrodes. While the atomic configuration at the BTO/SRO interface is well defined due to the continuation of the crystal structure, the BTO/Pt interface may adopt a variety of different structures,[6] leading to strongly different screening behavior. In addition, metal deposition often leads to formation of defects at the interface,[7–11] which may also modify the screening behavior substantially.

Experimental evidence for the dependence of Schottky barrier height on polarization is provided by leakage current measurements of ferroelectric $Pb(Zr,Ti)O_3$ thin films[12,13] and by electrical currents through ferroelectric tunnel junctions.[14–18] However, extraction of quantitative values for the Schottky barrier heights and their dependence on polarization requires model assumptions on charge transport. In addition, leakage current behavior often depends crucially not only on electrode material but also on the details of electrode preparation. A microscopic understanding of this dependence may be facilitated by a more extensive knowledge on Schottky barrier heights and their dependence on applied voltage and/or polarization.

The determination of Schottky barrier heights using x-ray photoelectron spectroscopy (XPS) is typically performed using interface experiments. The approach is possible since binding energies in XPS are calibrated with respect to the Fermi energy of the spectrometer, which is aligned with the Fermi energy of the sample by an electric contact. From a clean (semiconducting) substrate one obtains the binding-energy of the valence-band maximum E_{VB} with respect to the Fermi level as well as the core-level binding energies. The binding-energy difference between the valence-band maximum and any core level is a material constant, which remains constant upon interface formation.[19,20] Once the binding-energy difference between the valence-band maximum and a core-level is known for a material, it is possible to extract the Fermi-level position in the band gap directly from the core-level binding energy. Following the evolution of the core-level binding energies during interface formation by stepwise deposition of a contact material, the Fermi-level position at the interface is directly obtained. For semiconductor/metal interfaces, the Fermi-level position at the interface corresponds, by definition, to the Schottky barrier height. Such photoemission interface experiments have been extensively used since the late 70s of the last century to understand Schottky barrier formation of semiconductor materials (see, e.g., Refs. 21–26). In the case of metal contacts, the barrier formation is in most cases completed after deposition of one monolayer. For conventional semiconductors, also quantitative agreement with barrier heights derived from electrical measurements has been obtained.[21]

In previous work, we have addressed Schottky barrier formation and energy-band alignment of perovskite oxides using

XPS and typical interface experiments, which are performed by repeated deposition-analysis cycles with stepwise increase of the overlayer thickness.[8–11,27–31] Even for polycrystalline Pb(Zr,Ti)O_3 (PZT) ceramics, which should exhibit a variety of polarization orientations at the interface, a unique Schottky barrier height has been derived.[29] This is indicated by the sharp and symmetric shape of the substrate core-levels after interface formation, since different Schottky barrier heights should give rise to different core-level binding energies as outlined above. The unique Schottky barrier height observed in the interface experiment with polycrystalline PZT may be interpreted in terms of a barrier height which does not depend on polarization. However, it may also be that the polarization components perpendicular to the interface disappear in the course of interface preparation, e.g., by the formation of closure domains.[32,33] In order to resolve this uncertainty it is necessary to perform Schottky barrier measurements with independent control of the polarization state of the sample.

In the present work, x-ray photoelectron spectroscopy (XPS) is used to determine absolute values of the Schottky barrier heights at interfaces of (100) oriented $BaTiO_3$ single crystals with RuO_2 and Pt electrodes in dependence on ferroelectric polarization. In extension of the previous work, the experimental approach described in this contribution enables us to directly obtain the dependence of barrier height on polarization by *in situ* control of the polarization state. As common for the determination of Schottky barrier heights using photoelectron spectroscopy, the approach provides direct, quantitative, and parameter-free values.

II. EXPERIMENT

In the present work, we have used the experimental arrangement depicted in Fig. 1 in order to follow changes in core-level binding energies upon applying electric fields across the sample. In contrast to a typical interface experiment, where the thickness of the electrode material is systematically

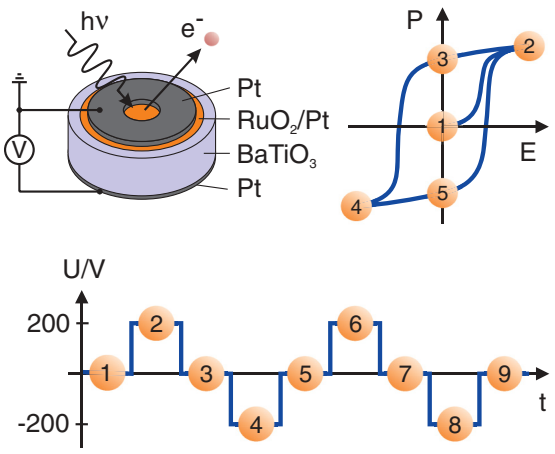

FIG. 1. (Color online) (a) Arrangement of layers and electric contacts for measurement of polarization dependence of Schottky barrier heights; (b) schematic polarization field loop for ferroelectric samples starting from an unpoled state (1); (c) the function of the voltage applied on the sample for XPS analysis.

increased to follow the evolution of the chemical and electronic interactions at the interface, the electrode thickness has not been varied during the experiment in this arrangement. As outlined above, the barrier height can be determined directly from the core-level binding energies once the binding-energy difference between the core-level and the valence-band maximum is known. For the present work, these binding-energy differences are taken from a large set of samples independent from the present experiment.

The application of an electric field requires attachment of an electric contact to the top electrode. The area of the top electrode also needs to be confined in order to avoid a short circuit to the bottom electrode. To monitor the barrier heights using XPS, the top metal electrode must be sufficiently thin ($\lesssim$3 nm) to allow a fraction of photoelectrons from the ferroelectric substrate to transverse the metal film without energy loss. On the other hand, the electrode must be thick enough in order to provide a continuous layer for electric contact. In previous experiments using polycrystalline PZT ceramics with rough surfaces, we have found that a RuO_2 electrode layer of 1.5 nm thickness is sufficient to remove the charging observed in the XPS experiment, i.e., it provides a continuous and conducting layer.[29] In the present case, where flat single-crystal $BaTiO_3$ samples are used, the conductivity of the RuO_2 layer should also be sufficient to provide the electric contact, which is necessary to allow the BTO to switch polarization when sufficiently large voltages are applied. In the case of Pt electrodes, we have also observed layerlike growth providing a continuous and conducting film for thickness well below 2 nm.[9] In order to ensure conductivity over the whole contact area, we have applied a secondary 50-nm-thick electrode layer of Pt. A circular hole with a diameter of 1 mm in the center of the secondary layer was prepared using a lithographically structured photoresist. The photoresist was finally removed with acetone to expose the thin electrode in the center.

As ferroelectric samples 0.4-mm-thick $BaTiO_3$ single crystals purchased from Crystec (Berlin, Germany) have been used. Single crystals have been chosen for the experiment instead of thin films to avoid problems with short circuits, which are likely to appear on thin films due to the large area (several mm^2) of the electrodes required for the experiment. Due to the low carrier mobility of undoped $BaTiO_3$,[34] leakage currents through the 0.4-mm-thick sample would be bulk dominated and too small to be measured. A correlation of barrier heights with electrical measurements has therefore not been possible. Before electrode deposition the crystals were heated to 400 °C in the deposition chamber in 2 Pa oxygen atmosphere for 1 h. This treatment effectively removes adsorbates like hydrocarbons and water and results in a contamination-free surface.[29,35] One side of the crystals was then coated with 50 nm Pt, while the other was first coated with either a ~3-nm-thick RuO_2 or Pt layer, resulting in two different samples with Pt/BTO/RuO_2 and Pt/BTO/Pt electrode structure. Pt and RuO_2 deposition were performed using dc and reactive rf magnetron sputtering at room temperature, respectively.[9,27] The crystalline structure of the films on the BTO single-crystal surface is not known. The RuO_2 films prepared by reactive sputtering at room temperature are fully oxidized and exhibit a work function of ~6.1 eV and an electric

resistivity of $\sim 10^{-4}\ \Omega\,\mathrm{cm}$.[27] Typical obtained work functions of Pt films are ~5.6 eV.[9]

The samples were mounted on a sample holder consisting of two electrically isolated sections, which were wired to the plane bottom and the structured top electrode, respectively. In the spectrometer system (Physical Electronics PHI 5700), the two parts of the sample holder are separately wired to the manipulator. Binding energies of the spectrometer are independently calibrated using a sputter cleaned metallic Ag foil.

X-ray photoelectron spectra were recorded in order to position the sample and to monitor the state of the as-prepared sample before applying any voltage. Apart from the carbon and oxygen signals, the survey spectra showed mostly Ru (for the sample with RuO_2 top electrode) and Pt but also weak Ba and Ti emissions from the $BaTiO_3$ substrate. All emissions exhibit sharp peak shapes (see Fig. 3), indicating that no sample charging is present, i.e., that the top electrode provides a continuous contact. During XPS measurement, the top electrode was connected to ground, which provides the Fermi-level binding-energy reference of the spectrometer. Due to application of the voltage to the bottom electrode, no binding-energy shifts of the top electrode are expected with applied voltage. A positive voltage applied to the bottom electrode then corresponds to a polarization of the $BaTiO_3$ pointing towards the top contact, which is the one where changes of the barrier height are monitored by XPS. The sequence of voltages applied during the measurement is shown in Fig. 1.

Hysteresis curves were recorded after performing the XPS measurement of the as-prepared sample with the sample maintained in the spectrometer system. A home-made Sawyer-Tower circuit with a reference capacitance of 4.7 μF and triangular voltage profiles have been used. Sample grounding was removed during the measurement. The same high-voltage amplifier with a short-circuited reference capacitor was used to apply voltages during XPS measurement.

III. RESULTS AND DISCUSSION

The hysteresis loops obtained from the Pt/BTO/RuO_2 and Pt/BTO/Pt samples are shown in Fig. 2. Each loop was measured at 100 mHz with two sweeps. Maximum voltages of ± 200 V were applied, corresponding to electric fields of ± 5 kV/cm, which is higher than the coercive field of $BaTiO_3$ of 1 kV/cm.[1] While the coercive fields extracted from Fig. 2 correspond to those of $BaTiO_3$, the remanent and saturated polarization are significantly lower than the bulk polarization of 25 μC/cm^2.[1]

Measurements performed with the same setup on poly-crystalline PZT and La-doped PZT (PLZT) ceramics with Pt and RuO_2 electrodes prepared as the ones applied here have shown hysteresis curves with shape, coercive field, and polarization comparable to those measured in a separate setup with commercial fired Ag electrodes. The fatigue behavior of PZT ceramics up to 10^6 cycles has also been found to be largely identical for all our electrode materials.[29] We therefore attribute the reduced polarization in Fig. 2 at least partially to the quality of the single crystals, rather than to that of the electrode preparation or to an artefact of the measurement

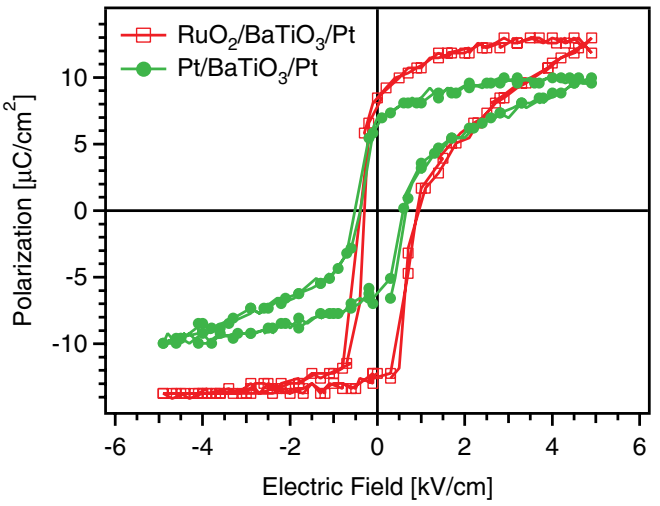

FIG. 2. (Color online) Polarization-electric field loops of the $BaTiO_3$ single crystals recorded with the sample mounted in the spectrometer.

setup. The reduced polarization may be caused by incomplete domain switching, e.g., by defects at or near the interface. This may be particularly the case for the Pt electrodes, which show poor saturation of polarization with increasing field (see Fig. 2). Nevertheless, despite the uncertainty in the polarization state of the crystal, the hysteresis curves shown in Fig. 2 provide sufficient evidence for polarization of the crystal.

In order to study the influence of polarization on the XPS binding energies, the voltage at the bottom electrode was sequentially set to constant values of $+200$, 0, -200, and 0 V. For each voltage step a set of Ba $3d$, Ti $2p$, Ru $3d$ (for the Pt/BTO/RuO_2 sample), and Pt $4f$ core-levels was recorded. Due to the very low signal intensity, the Ti $2p$ spectra were not recorded for the 0-V steps, which correspond to the remanent polarization state. The complete voltage cycle was repeated in order to verify the reproducibility of the observed shifts. The spectra recorded for the experiment with RuO_2 and Pt top electrodes are shown in Fig. 3.

A significant decrease of intensity is observed for the Ba $3d$ spectra of the Pt/BTO/Pt sample when a negative voltage is applied to the bottom electrode. This observation comes along with a general reduction of the intensity of photoelectrons with lower kinetic energy. The reduction is completely reversible and therefore tentatively attributed to the modification of the analyzer transmission function by the applied voltage. It is less pronounced for the Pt/BTO/RuO_2 sample, probably due to a slightly different geometrical arrangement of the sample holder in front of the entrance slit of the electron analyzer's lens system.

Independent on the applied voltage, the core-levels of the top electrode material exhibits constant shape and a binding energy of either 281.05 eV (RuO_2) or 71.05 eV (Pt), which are characteristic for metallic RuO_2 and Pt, respectively.[9,10,27,29] As the binding energies in XPS are measured with respect to the Fermi level of the spectrometer system, this confirms that the complete top electrode layers are electrically connected to ground during the whole measurement cycle. In the case of the RuO_2 top electrode, the secondary thick Pt electrode also exhibits a binding-energy of 71.05 eV. Consequently,

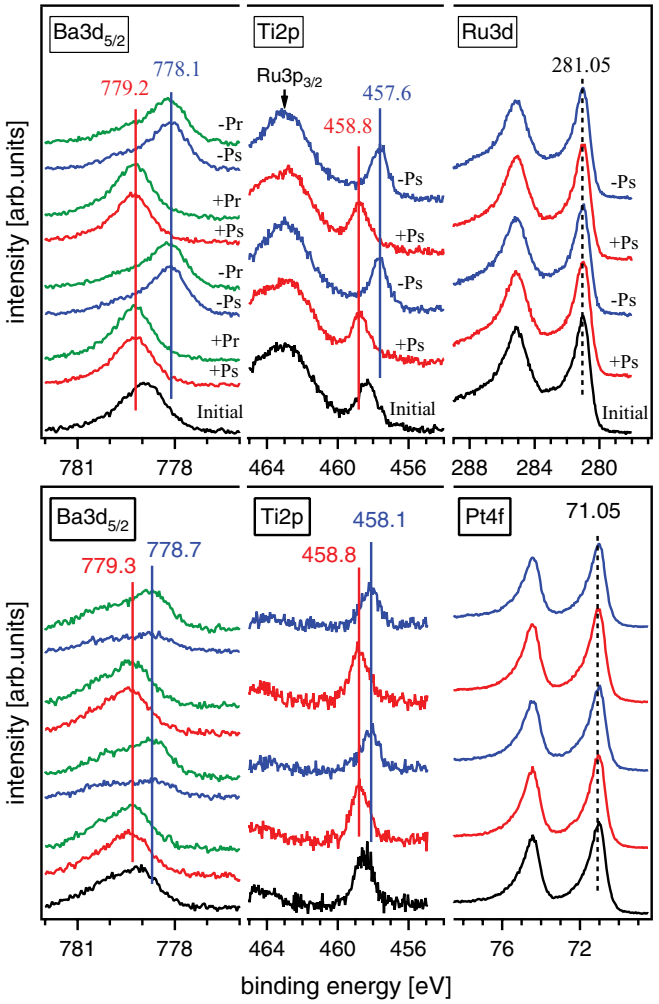

FIG. 3. (Color online) Core-level spectra of $BaTiO_3$ single crystals with RuO_2 (upper row) and Pt (lower row) top electrodes in dependence on applied voltage. The voltage applied across the samples are 0 V for the initial and remanent states (±Pr), +200 V for positive saturation (+Ps), and −200 V for negative saturation (−Ps), respectively. In all cases, the top electrode was electrically connected to the spectrometer system and the voltage was applied to the bottom electrode. The color codes for the upper and lower set of spectra are identical.

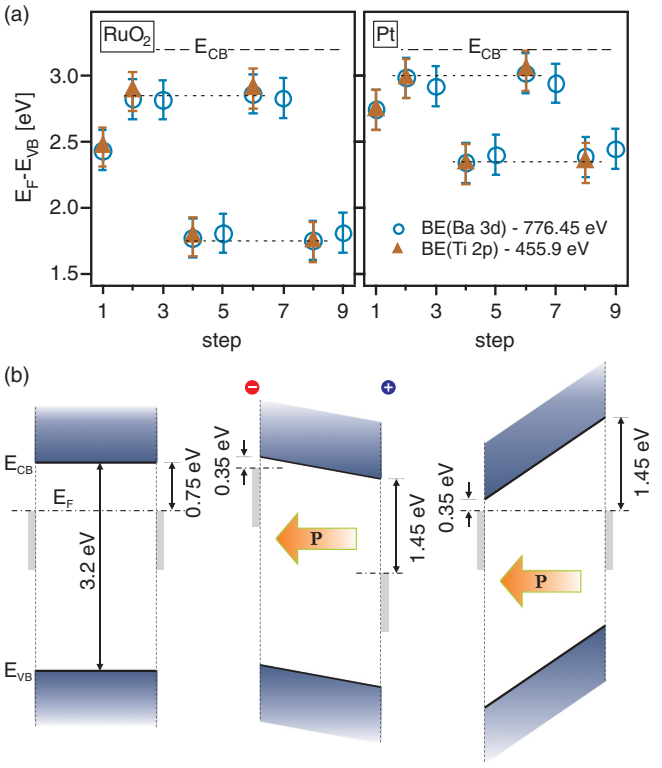

FIG. 4. (Color online) (a) Valence-band maximum energy with respect to the Fermi level as obtained from Ba 3*d* and Ti 2*p* core-level binding energies recorded during voltage switching with RuO_2 and Pt electrodes. (b) Schematic energy diagrams with two RuO_2 electrodes before (left), during (middle), and after poling (right). The arrows indicate the direction of polarization. For simplicity, two identical electrodes have been chosen.

the Fermi level of the spectrometer is verified to provide the binding-energy reference in our experiment, which is required for interpreting binding-energy shifts of the BTO-related emissions in terms of changes in Schottky barrier height.

The Ba 3*d* and Ti 2*p* core-levels of the as-prepared Pt/BTO/RuO_2 sample exhibit binding energies of 778.9 ± 0.1 and 458.35 ± 0.1 eV, respectively. In $BaTiO_3$, the binding-energy differences between the valence-band maximum and the Ba 3*d* and the Ti 2*p* core-levels amount to 776.45 ± 0.1 and 455.9 ± 0.1 eV, respectively. These values are derived from a large set of different $BaTiO_3$ and (Ba,Sr)TiO_3 thin films deposited onto conducting substrates. The Ba 3*d* and Ti 2*p* binding energies of the as-prepared sample hence correspond to a Fermi level at the $BaTiO_3/RuO_2$ interface of $E_F - E_{VB} = 2.45 \pm 0.15$ eV above the valence-band maximum E_{VB}. This is very close to the value of $E_F - E_{VB} = 2.35$ eV, reported for the (Ba,Sr)TiO_3/RuO_2 interface,[27] and indicates the good reproducibility of the measurement. The same holds for the Pt/BTO/Pt interface, where the as-prepared sample exhibits a Fermi-level position $E_F - E_{VB} \approx 2.6$ eV, in close agreement with measurements of interfaces between $BaTiO_3$ films and Pt.[36]

In contrast to the core-levels of the metallic RuO_2 or Pt electrodes, the Ba 3*d* and Ti 2*p* core-levels show pronounced reversible shifts with applied voltage. As the binding-energy shifts of the Ba 3*d* and Ti 2*p* core-levels are of the same magnitude (see also Fig. 4), it is straightforward to attribute the shifts to changes of the Fermi level with respect to the band edges, which correspond to changes of the Schottky barrier heights at the interfaces.

In any of the recorded states of the Pt/BTO/RuO_2 interface, the shape and the width of the BTO core-levels remain unchanged. This indicates a laterally homogeneous Fermi-level position, i.e., a homogeneous barrier height.[29] Due to the obvious dependence of barrier height on polarization, this provides evidence that the polarization of $BaTiO_3$ at the BTO/RuO_2 interface is mostly homogeneous during all experimental steps. This is surprising, as the polarization of the crystal (see Fig. 2) is significantly lower than expected,[1] indicating that part of the polarization does not switch.

In contrast to the BTO/RuO_2 sample, the spectra recorded at the BTO/Pt interface of the Pt/BTO/Pt sample show noticeable

changes of peak shape with applied voltage. The Ti $2p$ emission, e.g., becomes clearly asymmetric with polarization of the sample and the asymmetry is always towards the peak position of the initial state. The asymmetry may be explained in two different ways: (i) Polarization occurs only at a part of the contact area, i.e., switching does not fully polarize the sample or (ii) the screening (i.e., λ_{eff}) of the polarization by the Pt metal and therefore $\Delta\Phi_B$ [see Eq. (1)] are laterally inhomogeneous. The latter may be caused by a lateral variation of the interfacial atomic configuration. As predicted by Stengel and co-workers,[3,4] the screening can be very efficient for certain configurations of the BTO/Pt interface. In this case, no variation of barrier height with polarization is to be expected. An inhomogeneous screening and barrier formation at the BTO/Pt interface, in contrast to a homogeneous barrier formation at the BTO/RuO_2 interface, may also be induced by an inhomogeneous concentration of defects at the BTO/Pt interface. Generation of defects has been observed during Pt deposition onto a variety of oxides[7,9,10] and is likely to occur also at the BTO/Pt interface.

The binding energies for the as-prepared interfaces are in between the values found for the two different polarization directions and agree with values measured in experiments where the electrode was stepwise deposited onto a clean surface.[27,36] This indicates that barrier heights determined in interface experiments with photoemission using unintentionally poled ferroelectrics[10,28] do not correspond to a situation with significant polarization perpendicular to the interface. The presence of a noticeable fraction of domains polarized either towards or away from the interfaces is therefore ruled out for the as-prepared interfaces.

After polarization of the sample in either direction, the Ba $3d$ and Ti $2p$ core-levels exhibit only small changes with shifts $\lesssim$0.1 eV after the removal of the voltage. A slight change of barrier height towards the unpoled state is to be expected, as the remanent polarization is lower than the saturated polarization. The small changes of binding energies (barrier heights) indicate, however, that the polarization remains largely present in the course of the photoemission measurement after removal of the voltage, in good agreement with the hysteresis loop. It also indicates that the photoemission process, which leads to significant generation of electron-hole pairs,[9,23] has no strong influence on the polarization state of the sample. It is therefore unlikely that the absence of polarization found for the as-prepared interfaces (see above), is an artefact induced by the photoemission process.

In order to quantify the changes of the Schottky barrier height with polarization, the binding energies of the Ba $3d$ and Ti $2p$ core-levels are plotted for the different voltage steps in Fig. 4(a). By subtracting the binding-energy differences between the core-levels and the valence-band maximum given above, the plot directly reveals the Fermi-level position at the interface with respect to the $BaTiO_3$ valence-band maximum. These values are equivalent to the Schottky barrier height for holes. The Schottky barrier heights for electrons are obtained by subtracting the hole barriers from the band gap. As is evident from Fig. 4(a), both Ba $3d$ and Ti $2p$ core-levels reveal the same dependence of barrier height with polarization. A polarization pointing towards (away from) the top electrode interface, corresponding to a positive (negative) voltage at the bottom electrode as in steps 2 and 6 (steps 4 and 8), leads to an upward (downward) shift of the Fermi level at the top electrode. It should be mentioned that the direction of the shift agrees with the theoretically expected change of barrier height with polarization.[5]

For the BTO/RuO_2 interface, the Fermi-level positions at the interface for polarization pointing towards and away from the interface are derived as $E_F - E_{VB} = 2.85 \pm 0.15$ eV and 1.75 ± 0.15 eV, respectively. A very similar behavior but with different values for the Schottky barrier heights of 2.9 ± 0.15 eV for polarization pointing towards the interface and of 2.25 ± 0.15 eV for polarization pointing away from the interface are obtained for the BTO/Pt sample, as shown in the right graph of Fig. 4(a).

The difference in barrier height with polarization reversal of $\Delta\Phi_B = 1.1$ eV for the RuO_2 electrode is smaller than the change of 1.8 eV predicted by DFT for the $BaTiO_3/SrRuO_3$ interface,[5] but of similar magnitude. A quantitative agreement between theory and experiment is not expected, as the screening length for the $BaTiO_3/SrRuO_3$ interface will be different from the BTO/RuO_2 interface due to the epitaxial nature of the former and the different crystal and electronic structures of $SrRuO_3$ and RuO_2.

For the Pt electrodes, the change of barrier height with polarization amounts to $\Delta\Phi_B = 0.65$ eV, which is much larger than the variation predicted for the very short effective screening length calculated for a Pt_2/BaO interface configuration.[4] As already argued above, the large difference can be attributed to a different atomic configuration at the interface, or to the presence of defects. The concentration of defects at an oxide/Pt interface can vary significantly with chemical oxidation or reduction leading to changes of the barrier height of up to 1 eV.[7,9,10] While it is not expected that the reversible change of barrier height upon polarizing the sample reported here is caused by a reversible change of oxygen vacancy concentration, an influence of the defects on the macroscopic polarization and microscopic screening length is likely.

In order to gain more insights into the role of defects on the screening behavior, it would be necessary to independently control the defect concentration. So far, we have not been able to chemically modify the BTO/Pt interface in the setup described in Fig. 1. The main obstacle is that any postdeposition annealing in oxidizing or reducing atmosphere, which would reduce or increase the oxygen vacancy concentration at the interface, leads to island formation of the thin top electrode layer.[9] With such discontinuous electrodes, polarization switching would no more be possible. In addition, charging of the insulated parts of the surface would prevent the determination of barrier heights. A way out of this dilemma may be to use thicker top electrodes in combination with high kinetic-energy XPS, which provides two to five times larger information depths than normal XPS.

Additional experiments using the arrangement sketched in Fig. 1 have been performed with a $SrTiO_3$ single-crystal and polycrystalline PZT and PLZT ceramics. No significant changes of core-level binding energies are observed for the $SrTiO_3$ single-crystal sample with applied voltage. The P(L)ZT ceramics have been polished to a thickness <300 μm, such that the maximum voltage of $\pm$300 V is sufficient to pole the samples. The experiments with P(L)ZT showed largely

identical behavior in dependence on applied voltage compared to the one reported here. The binding-energy changes are also of similar magnitude. It is noted that polarization is naturally inhomogeneous at the interface for the polycrystalline P(L)ZT samples. Consequently, significant changes in core-level line shape are observed with poled samples. However, the unpoled samples also exhibit sharp emission lines, indicating absence of polarization components perpendicular to the interface as discussed above for the BTO samples (see also Ref. 29). These experiments confirm the interpretation of the above described binding-energy shifts in terms of a polarization dependence of barrier height.

IV. SUMMARY AND CONCLUSION

In the present work it has been demonstrated how photoelectron spectroscopy can be used to obtain so far unaccessible information on the properties of ferroelectric interfaces. Direct and quantitative measurements of Schottky barrier heights in dependence on ferroelectric polarization are obtained, giving direct support for theoretical predictions and models explaining polarization dependent current-voltage characteristics in terms of polarization dependent Schottky barrier heights. The experimental procedure is exemplified for $BaTiO_3$ single crystals with metallic RuO_2 and Pt electrodes. Despite the incomplete polarization of the used $BaTiO_3$ single crystals, significant variation of barrier height with polarization of $\Delta\Phi_B = 1.1$ eV and $\Delta\Phi_B = 0.65$ eV is observed with RuO_2 and Pt electrodes, respectively. With Pt electrodes, an asymmetric change of the photoemission core-levels is observed, which is attributed to laterally inhomogeneous polarization. The magnitude of the barrier variation cannot be considered as being intrinsic for a given ferroelectric and electrode combination, as the effective screening length λ_{eff} can strongly depend on interface preparation. The outlined measurement procedure can be used to study the effects of interface preparation on the polarization dependence. It may be used to unravel the influence of interfacial defects on the polarization of ferroelectric materials. Such defects may be responsible for the inhomogeneous polarization at the $BaTiO_3$/Pt interface.

ACKNOWLEDGMENT

This work was supported by the German Science Foundation (DFG) within the collaborative research center SFB 595 (Electrical Fatigue of Functional Materials).

*Present address: High Magnetic Field Lab, Hefei Institutes of Physical Science, Chinese Academy of Sciences (CAS), Shushanhu Road 350, Hefei 230031, China.

[1] A. J. Moulson and J. M. Herbert, Electroceramics, 2nd ed. (John Wiley & Sons, Chichester, 2003).
[2] M. E. Lines and A. M. Glass, *Principles and Applications of Ferroelectrics and Related Materials* (Clarendon, Oxford, 1977).
[3] M. Stengel and N. A. Spaldin, Nature (London) **443**, 679 (2006).
[4] M. Stengel, D. Vanderbilt, and N. A. Spaldin, Nat. Mater. **8**, 392 (2009).
[5] M. Stengel, P. Aguado-Puente, N. A. Spaldin, and J. Junquera, Phys. Rev. B **83**, 235112 (2011).
[6] F. Rao, M. Kim, A. J. Freeman, S. Tang, and M. Anthony, Phys. Rev. B **55**, 13953 (1997).
[7] C. Körber, S. P. Harvey, T. O. Mason, and A. Klein, Surf. Sci. **602**, 3246 (2008).
[8] R. Schafranek and A. Klein, Solid State Ionics **177**, 1659 (2006).
[9] R. Schafranek, S. Payan, M. Maglione, and A. Klein, Phys. Rev. B **77**, 195310 (2008).
[10] F. Chen, R. Schafranek, W. Wu, and A. Klein, J. Phys. D: Appl. Phys. **42**, 215302 (2009).
[11] F. Chen, R. Schafranek, W. Wu, and A. Klein, J. Phys. D: Appl. Phys. **44**, 255301 (2011).
[12] L. Pintilie, I. Vrejoiu, D. Hesse, G. LeRhun, and M. Alexe, Phys. Rev. B **75**, 104103 (2007).
[13] D. Lee, S. H. Baek, T. H. Kim, J.-G. Yoon, C. M. Folkman, C. B. Eom, and T. W. Noh, Phys. Rev. B **84**, 125305 (2011).
[14] V. Garcia, S. Fusil, K. Bouzehouane, S. Enouz-Vedrenne, N. D. Mathur, A. Barthélémy, and M. Bibes, Nature (London) **460**, 81 (2009).
[15] A. Gruverman, D. Wu, H. Lu, Y. Wang, H. W. Jang, C. M. Folkman, M. Y. Zhuravlev, D. Felker, M. Rzchowski, C.-B. Eom, and E. Y. Tsymbal, Nano Lett. **9**, 3539 (2009).
[16] P. Maksymovych, S. Jesse, P. Yu, R. Ramesh, A. P. Baddorf, and S. V. Kalinin, Science **324**, 1421 (2009).
[17] A. Crassous, V. Garcia, K. Bouzehouane, S. Fusil, A. H. G. Vlooswijk, G. Rispens, B. Noheda, M. Bibes, and A. Barthélémy, Appl. Phys. Lett. **96**, 042901 (2010).
[18] D. Pantel, S. Goetze, D. Hesse, and M. Alexe, ACS Nano **5**, 6032 (2011).
[19] E. A. Kraut, R. W. Grant, J. R. Waldrop, and S. P. Kowalczyk, Phys. Rev. B **28**, 1965 (1983).
[20] S. A. Chambers, T. Droubay, T. C. Kaspar, M. Gutowski, and M. van Schilfgaarde, Surf. Sci. **554**, 81 (2004).
[21] P. W. Chye, I. Lindau, P. Pianetta, C. M. Garner, C. Y. Su, and W. E. Spicer, Phys. Rev. B **18**, 5545 (1978).
[22] L. J. Brillson, C. F. Brucker, A. D. Katnani, N. G. Stoffel, R. Daniels, and G. Margaritondo, Surf. Sci. **132**, 212 (1983).
[23] M. Alonso, R. Cimino, and K. Horn, Phys. Rev. Lett. **64**, 1947 (1990).
[24] G. Margaritondo, Rep. Prog. Phys. **62**, 765 (1999).
[25] H. Ishii, K. Sugiyama, E. Ito, and K. Seki, Adv. Mater. **11**, 605 (1999).
[26] Y. Gao, Mater. Sci. Eng. R **68**, 39 (2010).
[27] R. Schafranek, J. Schaffner, and A. Klein, J. Eur. Ceram. Soc. **30**, 187 (2010).
[28] F. Chen, R. Schafranek, S. Li, W. Wu, and A. Klein, J. Phys. D: Appl. Phys. **43**, 295301 (2010).
[29] F. Chen, R. Schafranek, A. Wachau, S. Zhukov, J. Glaum, T. Granzow, H. von Seggern, and A. Klein, J. Appl. Phys. **108**, 104106 (2010).

[30]R. Schafranek, S. Li, F. Chen, W. Wu, and A. Klein, Phys. Rev. B **84**, 045317 (2011).
[31]A. Klein, Thin Solid Films **520**, 3721 (2012).
[32]P. Aguado-Puente and J. Junquera, Phys. Rev. Lett. **100**, 177601 (2008).
[33]C.-L. Jia, K. W. Urban, M. Alexe, D. Hesse, and I. Vrejoiu, Science **331**, 1420 (2011).
[34]F. D. Morrison, P. Zubko, D. J. Jung, J. F. Scott, P. Baxter, M. M. Saad, R. M. Bowman, and J. M. Gregg, Appl. Phys. Lett. **86**, 152903 (2005).
[35]Y. Gassenbauer, R. Schafranek, A. Klein, S. Zafeiratos, M. Hävecker, A. Knop-Gericke, and R. Schlögl, Phys. Rev. B **73**, 245312 (2006).
[36]E. Arveux, Ph.D. thesis, Université de Bordeaux I, Bordeaux, 2009.